Two Birds, One Stone: Microsecond Dark Excited-State Lifetime and Large Cage Escape Yield afforded by an Iron-Anthracene Molecular Dyad

Felix Glaser,[‡,*] Simon De Kreijger[‡] and Ludovic Troian-Gautier[‡,ϕ*]

[‡] UCLouvain, Institut de la Matière Condensée et des Nanosciences (IMCN), Molecular Chemistry, Materials and Catalysis (MOST), Place Louis Pasteur 1/L4.01.02, B-1348 Louvain-la-Neuve, Belgium

[ϕ]Wel Research Institute, Avenue Pasteur 6, 1300 Wavre, Belgium

KEYWORDS. Cage Escape Yields • Iron • Energy Transfer • Lifetime • Earth Abundant

ABSTRACT: Iron photosensitizers represent a holy grail in photochemistry, but their widespread implementation is limited by their short excited-state lifetimes and poor cage escape yields. Here, the introduction of an anthracene moiety appended to an iron(III) complex allows to solve both limitations and generate a novel dyad exhibiting an extraordinary excited-state lifetime of 11.5 µs. The key to achieve this remarkably long lifetime is the depopulation of the short-lived iron-centered emissive excited state to populate a dark triplet state located on the anthracene-like moiety with a spin-forbidden deactivation. Population of the triplet anthracene only occurs with ~10% efficiency in acetonitrile but still allows to expand the scope of reactivity accessible with iron-based photosensitizers, which now encompasses energy transfer to $^3O_2$. In addition, in a proof-of-principle investigation with methyl viologen as electron acceptor, the population of a triplet excited state allows a drastic 10-fold increase of the cage escape yield from 4.5% for the unsubstituted complex, to 42% for the molecular dyad. Hence, this new iron-based dyad provides a complementary approach for complexes based on first-row transition metals as alternatives to well-established analogues based on precious metals. We believe that further spectroscopic investigations and synthetic modifications of the energy acceptor and linkage to the photosensitizer will be key to use these innovative dyads for applications in the future.

INTRODUCTION

Photo(redox) catalysis established itself as a credible alternative for catalysis to use light instead of heat as energy source. Increased efforts have been made towards the development of photosensitizers based on earth-abundant metals as alternative to those based on precious metals like $[Ru(bpy)_3]^{2+}$ (bpy = 2,2-bipyridine) and *fac*-[Ir(ppy)$_3$] (ppy = 2-phenylpyridine).[1] Iron is an obvious alternative, but due to the smaller ligand field strength in 3d metal complexes compared to 4d and 5d analogues, new concepts and ligand design strategies are needed to achieve long-lived emissive excited states.[2-8] In 2017, a strategic change from Fe^{II} complexes with metal-to-ligand charge transfer (^{3*}MLCT) excited states to Fe^{III} complexes with ligand-to-metal charge transfer (^{2*}LMCT) excited states was pioneered by Wärnmark and co-authors.[9] Using this strategy, Wärnmark and co-authors developed in 2019 a Fe^{III} photosensitizer ($[Fe(L^{Ph})_2]^+$,[10] where L^{Ph} is phenyl[tris(3-methyl-imidazolin-2-ylidene)]borate), **Figure 1**, that is outstanding not only because of its 2 ns excited-state lifetime and photoluminescence quantum yield, but also because diffusion-controlled excited-state quenching became reachable, opening the door to applications in photoredox catalysis.[3, 10-15] Nevertheless, the 2 ns excited-state lifetime of $^{2*}[Fe(L^{Ph})_2]^+$ is considerably shorter than octahedral complexes based on second and third row transition metals. Hence, high concentrations with diffusion-limited quenching rate constants (k_q) are often needed to use this photosensitizer.[16] Consequently, strategies to increase this excited-state lifetime are still highly sought after.[2, 17-20]

Current strategies are either focusing on the adaption of concepts that were successfully established with 4d and 5d metal complexes and/or exploiting specific properties of the iron complexes through a deepened understanding of the excited-state landscape. Selected concepts to reach longer excited-state lifetimes of iron complexes that were recently investigated for Fe^{II} include, for example, the diastereoselective ion-pairing to manipulate spin-crossover dynamics,[21] the introduction of a triplet-triplet barrier to slow down deactivation processes,[22] or the modification of the second coordination sphere by protonation to influence MC and MLCT energies.[20]

In addition to these approaches, the development of less common ligand designs, when compared to photoactive complexes based on precious metals, was found to be beneficial for iron complexes to reach nanosecond excited-state lifetimes. Such strategy was used, for example, to introduce nested energy surfaces in a complex with a tetradentate macrocycle ligand and additional cyanide ligands,[17] to populate low-lying MLCT states by chelating cyclometalated phenylphenanthrolines,[19, 23] or to stabilize the ^{5}MC excited state in an iron complex with amido-based ligands.[24-26] Following on the latter example, a recent report on modification of the ligand structure also highlighted the ability to manipulate the excited-state decay pathways by intramolecular π-stacking to elongate the dark MC state within the nanosecond time range.[27] Overall, these

strategies all helped to enhance the excited-state lifetime of iron complexes, but were up to now also limited to reach at best a few nanoseconds.

For precious metal complexes, the lifetime of the ^{3*}MLCT excited states has been prolonged by introducing triplet energy acceptors as substituents in molecular dyads.[28-33] This concept, also called "triplet-reservoir effect", relies on an excited-state equilibrium between a metal complex and an attached triplet energy acceptor with an energy close to the emissive state of the metal.[28-34] Previous attempts to use similar approaches with iron complexes and attached polycyclic aromatic hydrocarbons (PAH) were unsuccessful to significantly enhance the excited-state lifetime of the bichromophore.[35-36] This is likely due to an energetic mismatch or a weak electronic coupling between the energy donor and acceptor moieties. An alternative to a repopulation of the MLCT state of the sensitizer has been investigated for iron complexes substituted by a zinc porphyrin.[37] While this approach allowed to populate microsecond-lived dark states for the chromophores based on Ru^{II} and Os^{II} centers,[38-39] it only lengthened the excited-state lifetime of the iron complexes within the picosecond to short nanosecond timescale.[37]

Another aspect to consider in excited-state reactivity is the cage escape yield (Φ_{CE}), i.e. the efficiency with which both radicals escape the solvent cage following bimolecular electron transfer.[12, 40-42] For $[Fe(L^{Ph})_2]^+$, it was shown that the reaction yields correlated with Φ_{CE}, that were much larger in dichloromethane than in acetonitrile.[12-13] Further studies indicated that this solvent trend is more generally applicable to this Fe^{III} photosensitizer.[42-43]

Herein, we introduced an anthracene moiety on the $[Fe(L^{Ph})_2]^+$ scaffold to harvest the excited-state energy from the iron sensitizer *via* doublet-triplet energy transfer (DTET),[44-49] thereby populating a dark triplet state of anthracene (^{3*}PhAn), expected to be significantly longer-lived than $[Fe(L^{Ph})_2]^+$ itself (**Figure 1**). During the evaluation of our manuscript, the bimolecular energy transfer of $[Fe(L^{Ph})_2]^+$ and anthracene derivatives *via* DTET was reported for application in sensitized triplet-triplet annihilation upconversion, confirming that this energy transfer is feasible.[49] Considerably, even with weak preaggregation between $[Fe(L^{Ph})_2]^+$ and anthracene derivatives detected at concentrations of 10 mM, less than 25% of the emissive ^{2*}LMCT excited state of iron are quenched, indicating that a bimolecular approach is not sufficient to efficiently depopulate the excited state of $[Fe(L^{Ph})_2]^+$.[49] On the other hand, this highlights again that a dyad might be an attractive alternative to circumvent the limitations set by diffusion and thus lead to excited-state depopulation within the picosecond timescale.[16, 50-51] In contrast to many approaches with 4d and 5d metal complexes that have used reservoir effects to reach tens of microsecond excited-state lifetime, we hypothesize that similar strategies for iron complexes are currently limited due to the much larger decay rate constant of the photosensitizer's excited state. As such, controlling this reservoir effect using iron photosensitizers is currently much more challenging to access significantly prolonged excited-state lifetimes. In our case, the developed strategy is to create an irreversible energy transfer to lead to a microsecond-lived dark state located on the energy acceptor. In addition, we hypothesized that the change in spin state of the excited state in a dyad through population of a ^{3*}PhAn will also be beneficial for Φ_{CE}. In fact, Olmsted and Meyer have shown that Φ_{CE} between methyl viologen and $[Ru(bpy)_3]^{2+}$ could be drastically improved by introducing an anthracene energy shuttle that accepted the energy of $^{3*}[Ru(bpy)_3]^{2+}$, thereby creating a pure ^{3*}An that led to spin-forbidden geminate charge recombination.[52] Herein, the proposed "*two birds, one stone*" approach is expected to increase both the excited-state lifetime and Φ_{CE}, thus efficiently expanding the applicability of Fe^{III} photosensitizer.

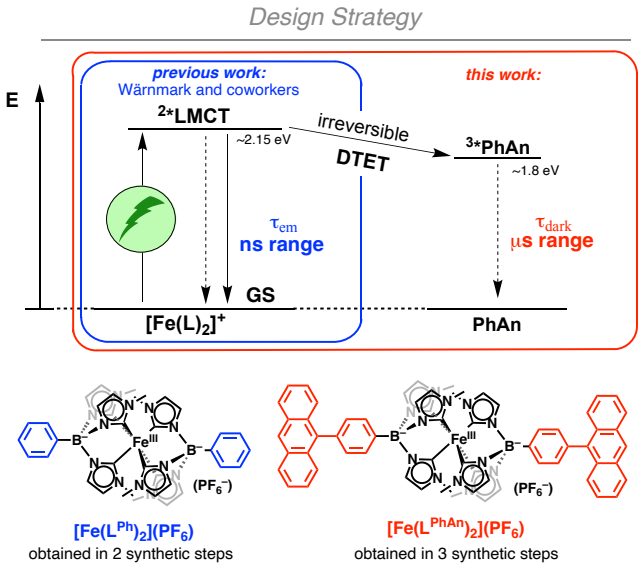

Figure 1. Energy scheme and structures of $[Fe(L^{Ph})_2]^+$ and $[Fe(^{LPhAn})_2]^+$. LMCT = ligand-to-metal charge transfer, DTET = doublet-to-triplet energy transfer, GS = ground state.

RESULTS AND DISCUSSION

The synthesis of $[Fe(L^{PhAn})_2]^+$ proceeded with only one additional step in comparison to the unsubstituted complex, namely *via* a Suzuki coupling reaction between the brominated complex $[Fe(L^{PhBr})_2]^+$, and 9-anthraceneboronic acid to generate the desired $[Fe(L^{PhAn})_2]^+$ in 52% yield (**Figure 1**). The purity of the compound was assessed by classical techniques that included ^{1}H NMR, high-resolution mass spectrometry and elemental analysis. In addition, UV-visible absorption spectroscopy (and spectroscopic deconvolution thereof), steady-state and time-resolved photoluminescence, excitation spectra as well as electrochemistry were in good agreement with a pure complex, as further detailed hereafter. The compound absorbed intensely in the UV region with a molar absorption coefficient of 19000 $M^{-1}cm^{-1}$ at 385 nm and appreciably at 503 nm with a molar absorption coefficient of 3500 $M^{-1}cm^{-1}$. The UV-visible absorption spectra of $[Fe(L^{PhAn})_2]^+$ (**Figure 2a**) was well modelled using a linear combination of the absorption spectrum of $[Fe(L^{Ph})_2]^+$ and twice the absorption spectrum of 9-phenylanthrancene (PhAn). The modelling provided a better fit when PhAn was used compared to unsubstituted anthracene (SI section 3.1.1), indicative of poor electronic coupling between the Fe-NHC scaffold and the phenyl ring.[53] This was also confirmed by electrochemistry where the reduction and oxidation potentials of the iron center and the attached 9-phenylanthracene are unaffected by the introduction of the energy acceptor moiety (SI section 3.1.2). Indeed, electrochemical characterisation of $[Fe(L^{Ph})_2](PF_6)$, $[Fe(L^{PhAn})_2](PF_6)$ and PhAn revealed only minor changes of the oxidation and reduction between the dyad and the individual components (**Table 1**). Measurements in acetonitrile and dimethylformamide indicate similar redox potentials in both solvents, although the iron-based reduction seems less reversible in acetonitrile than in dimethylformamide.

It is hypothesized that this is caused by the lower electrolyte concentration in acetonitrile that could only reach 25 mM before the photosensitizer precipitated. Overall, all of these photophysical characterisations are in line with an essentially decoupled system between the iron scaffold and the attached polyaromatic hydrocarbon.

Visible light excitation of $[Fe(L^{PhAn})_2]^+$ led to the prototypical photoluminescence of the $[Fe(L^{Ph})_2]^+$ core, albeit with smaller photoluminescence quantum yields, (1.17% *vs* 1.75%) as well as shorter emission lifetime (1.33 ns *vs* 2.05 ns). This change in emission properties is a first indication that the attachment of PhAn influences the excited-state decay pathway of the ^{2*}LMCT state, in line with the postulated energy transfer mechanism. However, the observation of photoluminescence reminiscent of $[Fe(L^{Ph})_2]^+$ also points towards an incomplete energy transfer.

Further information was garnered through the measurement of excitation spectra of both $[Fe(L^{Ph})_2]^+$ and $[Fe(L^{PhAn})_2]^+$, that were in good agreement with the molar absorption coefficient of the ground state absorption spectrum in acetonitrile (Figure S5). In addition, when the excitation of $[Fe(L^{PhAn})_2]^+$ occurred at 355 nm, i.e. in a region where >90% of the absorption is dominated by the PhAn moiety, the resulting detected anthracene-based emission around 400 nm is very weak and mainly iron-based emission is detectable (Figure S5). This presumably occurs *via* fast Förster Resonance Energy Transfer (FRET) and/or excited-state electron transfer quenching. Nevertheless, the weak emission around 400 nm is in perfect agreement with the emission of PhAn. This not only confirms that the iron core and the attached 9-phenylanthracene are electronically decoupled *via* the tetrasubstituted boron atoms, but also confirms the purity of $[Fe(L^{PhAn})_2]^+$ as the resulting emission is similar to PhAn and not similar to anthracene impurities.

Table 1. Electrochemical and Photophysical Data of $[Fe(L^{Ph})_2](PF_6)$, $[Fe(L^{PhAn})_2](PF_6)$ and PhAn.

PS	$E_{ox}(PS^{n/(n+1)})$ (V *vs* SCE)	$E_{red}(PS^{n/(n-1)})$ (V *vs* SCE)	$\lambda_{em,max}$ (nm)	$\Phi_{em,air}$ (%) [a]	$\Phi_{em,Ar}$ (%) [a]	$\tau_{0,air}$ (ns)	$\tau_{0,Ar}$ (ns)	$E_{0,0}$ (eV)
$[Fe(L^{Ph})_2]^+$	+0.68	–0.72	656	1.66 ±0.04	1.75 ±0.07	2.05	2.05	2.15 [b]
$[Fe(L^{PhAn})_2]^+$	+0.70, +1.35 [c]	–0.74, –2.00 [c]	655	1.14 ±0.02	1.17 ±0.01	1.33	1.33	2.15 [b]
PhAn	+1.33 [c]	–1.98 [c]	393, 415	- [d]	- [d]	- [d]	- [d]	~1.8 [e]

a) Photoluminescence quantum yields of iron complexes were determined relative to an aerated solution of $[Ru(bpy)_3](PF_6)_2$ in acetonitrile ($\phi = 0.018$).[54] b) The energies of the doublet excited states (for iron complexes) ($E_{0,0}$) were estimated based on the energy at the intersection of the normalized emission and absorption spectra. c) Non-reversible reduction or oxidation potential under these conditions. d) Not determined in this study. e) The triplet energy of PhAn was estimated based on the triplet energy of 9,10-diphenylanthracene (E_T ~1.77 eV).[55]

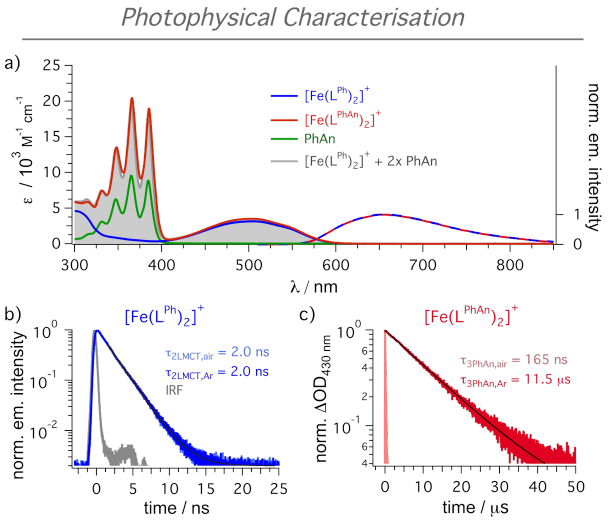

Figure 2. a) UV-vis absorption (solid) and emission (dashed) spectra of $[Fe(L^{Ph})_2]^+$ (blue), $[Fe(L^{PhAn})_2]^+$ (red) and PhAn (green) recorded in acetonitrile at room temperature. The simulated spectrum of the dyad by the sum of its components is shown in grey. Normalized excited-state lifetime of b) $[Fe(L^{Ph})_2]^+$ (blue, measured *via* time-resolved emission spectroscopy) and c) $[Fe(L^{PhAn})_2]^+$ (red, measured *via* time-resolved transient absorption spectroscopy) under air (light colors) and argon (dark colors). Spectroscopic details are presented in the supporting information in section 3.1.

The excited-state behavior of $[Fe(L^{PhAn})_2]^+$ was investigated in comparison to the unsubstituted $[Fe(L^{Ph})_2]^+$. First, the excited-state quenching of $[Fe(L^{Ph})_2]^+$ was investigated with increasing concentrations of PhAn in acetonitrile. Stern-Volmer analysis revealed a k_q of $1.0 \cdot 10^{10}$ $M^{-1}s^{-1}$, i.e. close to the diffusion limit of $2.0 \cdot 10^{10}$ $M^{-1}s^{-1}$.[56] Evidence for energy transfer was gained by nanosecond transient absorption spectroscopy where the absorption spectrum of ^{3*}PhAn was unambiguously observed (SI section 3.3). This species had a natural excited-state lifetime of ~50 µs under argon and 160 ns under air due to efficient energy transfer to $^3O_2$. Population of ^{3*}PhAn by bimolecular energy transfer is in agreement with the recent report by Wang and co-workers.[49] However, our quenching rate constant, measured in acetonitrile by time-resolved spectroscopy, is close to the diffusion limit, whereas the one reported by Wang and co-workers, measured by steady-state photoluminescence in DMSO, is above the diffusion limit by factors of ~25. This marked difference probably stems from ground-state pre-association in DMSO that were not disentangled from the steady-state quenching experiments. In our case, the dynamic excited-state lifetime quenching provides access to the diffusional quenching rate constant. Evaluation of static contributions indicated only a very small static quenching constant K_S of ~12 M^{-1} in acetonitrile (SI section 3.3.1), implying a small relevance of static contributions for the quenching with PhAn in acetonitrile.

Importantly, when $[Fe(L^{PhAn})_2]^+$ was investigated, similar transient absorption spectra were observed, confirming once again the population of the ^{3*}PhAn moiety with an excited-state lifetime of 11.5 µs (**Figure 2c**). This lifetime was also sensitive to the presence of oxygen and shortened to 165 ns in aerated acetonitrile, resulting in k_q ~$3 \cdot 10^9$ $M^{-1}s^{-1}$ with $^3O_2$ and an energy transfer efficiency >98%. It is important to note that the ΔAbs value of the ^{3*}PhAn signal in $[Fe(L^{PhAn})_2]^+$ is smaller than in the case of the bimolecular quenching and actinometric measurements indicate only ~10% of triplet state formation. This is probably caused by the incomplete triplet state population due to inefficient electronic coupling, in line with the remaining

photoluminescence disclosed previously, or to ultrafast reductive electron transfer from PhAn to $^{2*}[Fe(L^{PhAn})_2]^+$ that is thermodynamically feasible (SI section 3.6). Indeed, excited-state quenching via both energy or electron transfer are possible. Energy transfer from $^{2*}[Fe(L^{Ph})_2]^+$ ($E_{Doublet}$ = 2.15 eV) to 9-phenylanthracene ($E_{Triplet}$ = ~1.8 eV) is exergonic by about 0.35 eV. The exact triplet energy of 9-phenylanthracene is to the best of our knowledge not known and the value is estimated based on the triplet energy of the structurally closely related 9,10-diphenylanthracene ($E_{Triplet}$ = ~1.77 eV).[55] Alternatively, based on the ground-state reduction potential ($E_{1/2,red}$ = +0.68 V *vs* SCE) an excited-state reduction potential of $^{*}E_{1/2,red}$ = ~+1.47 V *vs* SCE is calculated. This state would thus also allow an exergonic excited-state oxidation of PhAn ($E_{1/2,ox}$ = +1.33 V *vs* SCE) by ~0.15 eV. From the bimolecular quenching studies for the excited-state quenching of $^{2*}[Fe(L^{Ph})_2]^+$ by 9-phenylanthracene (Figure S13) no photoproducts corresponding to reduced complex and/or oxidized 9-phenylanthracene were detected. Hence, contributions by an unproductive pathway with low cage escape yields and/or recombination below the nanosecond time-resolution of our instrument are possible and currently cannot be ruled out.

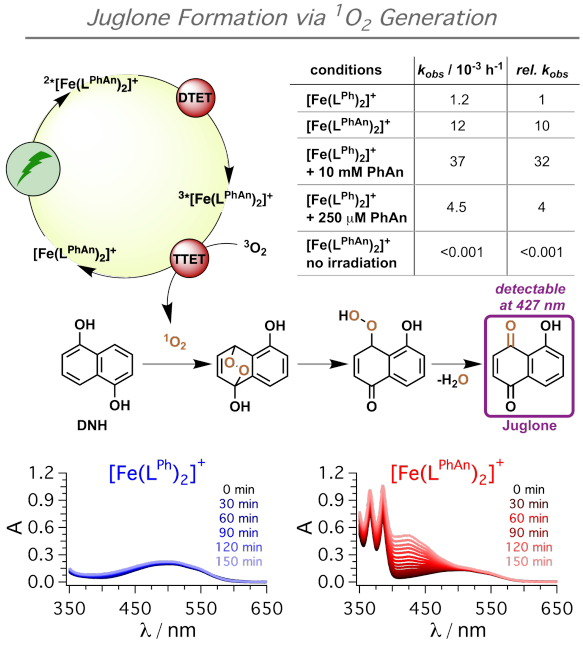

Figure 3. Green-light mediated $^1O_2$ production assessed *via* the conversion of 1,5-dihydroxynaphthalene (DHN) to Juglone (detected by UV-vis spectroscopy, $\lambda_{abs,max}$ = 427 nm). The proposed mechanism and tabulated observed rates for the different systems using [Fe(L^R)$_2$] (250 µM) with different conditions (top) and the UV-vis traces after different irradiation times for [Fe(L^{Ph})$_2$]$^+$ (blue) and [Fe(L^{PhAn})$_2$]$^+$ (red) measured in 2-mm cuvettes are provided (bottom, see also SI section 4 for further details). DTET = doublet-to-triplet energy transfer, TTET = triplet-to-triplet energy transfer.

To exploit the long excited-state lifetime, the photosensitized generation of $^1O_2$ was evaluated using the $^1O_2$-mediated oxidation of 1,5-dihydroxynaphthalene (DHN) to the corresponding 5-hydroxy-1,4-naphthalenedione (Juglone)[57-58] under LED irradiation (λ_{max} = 525 nm) (SI section 4). Due to its short excited-state lifetime, $[Fe(L^{Ph})_2]^+$ was unable to significantly produce $^1O_2$ and thus the conversion of DHN to Juglone is inefficient (**Figure 3**). $[Fe(L^{PhAn})_2]^+$ was able to generate Juglone more efficiently with an observed rate that is one order of magnitude larger (**Figure 3**). When $[Fe(L^{Ph})_2]^+$ and PhAn were used in 1:1 ratio at a concentration of 250 µM, the observed rate of Juglone formation was about 4 times faster compared to the system without anthracene, but also significantly slower than the dyad. The production of $^1O_2$ could be increased when $[Fe(L^{Ph})_2]^+$ was used with 10 mM of PhAn (**Figure 3**).[59] Thus, despite a ~10% triplet excited-state formation, the $[Fe(L^{PhAn})_2]^+$ dyad was still very competitive for $^1O_2$ formation.

We then turned to the investigation of Φ_{CE}, i.e. the efficiency with which radicals escape the solvent cage following bimolecular electron transfer.[40] For this, the model reaction of the oxidative quenching by methylviologen (MV^{2+}) was chosen. In acetonitrile, $^{2*}[Fe(L^{Ph})_2]^+$ was dynamically quenched by MV^{2+} with a k_q of $2.3\cdot10^9$ $M^{-1}s^{-1}$(**Figure 4a**). Despite a large quenching rate constant, Φ_{CE} in acetonitrile only reached 4.5%, in line with the initial report by Wärnmark(**Figure 4f** and SI section 3.5.1).[10] Strikingly, when $[Fe(L^{PhAn})_2]^+$ was used, a k_q of $1.4\cdot10^9$ $M^{-1}s^{-1}$ was determined (**Figure 4b**) with drastically increased Φ_{CE} to reach values of 42(±1)%, i.e. a one order of magnitude increase compared to the case of $[Fe(L^{Ph})_2]^+$ (**Figure 4f** and SI section 3.5.2). A comparison was then performed with ^{3*}PhAn that was first generated by energy transfer from $^{2*}[Fe(L^{Ph})_2]^+$. A concentration of 10 mM of 9-phenylantracene was used to reach a steady-state concentration of ^{3*}PhAn that was afterwards quenched by MV^{2+} *via* bimolecular electron transfer with a k_q of $4.3\cdot10^9$ $M^{-1}s^{-1}$. Φ_{CE} associated with the electron transfer from ^{3}PhAn to MV^{2+} reached 92(±2)% (**Figure 4f** and SI section 3.5.3). Thus, it appears that Φ_{CE} are drastically improved when an energy shuttle is introduced, either as a bimolecular arrangement, of *via* the formation of a dyad.

The difference in Φ_{CE} can be rationalized as follows (**Figure 5**): in the case of $[Fe(L^{Ph})_2]^+$, the geminate radical pair $^2\{Fe^{IV};MV^{\bullet+}\}$ exhibits a doublet character, and thus geminate charge recombination is spin-allowed leading to small Φ_{CE}.[10, 42] In the case of bimolecular reactivity between $[Fe(L^{Ph})_2]^+$ and PhAn that subsequently reacts with MV^{2+}, the geminate radical pair $^3\{PhAn^{\bullet+};MV^{\bullet+}\}$ exhibits a triplet character (**Figure S24**), and thus geminate charge recombination is spin-forbidden, leading to a Φ_{CE} of 92(±2)% (**Figure 4f** and SI section 3.5.3 and 3.6.3). In the case of the dyad, Φ_{CE} is 42(±1)% and this was counterintuitive as identical Φ_{CE} were expected.[60] A closer look at the transient absorption spectra indicates however that, in the case of the dyad, the hole on the oxidized PhAn moiety is efficiently transferred to the iron core (**Figure 4e**). Thus, three possible electronic configurations of the geminate radical pair can be represented (right part in **Figure 5**). Immediately after electron transfer, the electronic configuration of the iron core is back to its ground state configuration and the geminate radical pair more closely resembles a triplet configuration between the oxidized anthracene moiety and reduced methylviologen, i.e. $^3\{[Fe^{III}\text{-}PhAn^{\bullet+}];MV^{\bullet+}\}$. Spectroscopically, the formation of Fe^{IV} is observed as this hole transfer is energetically favorable by 0.6 eV (**Figure 4e**). In fact, two electronic configurations with an oxidized iron (Fe^{IV}) in the dyad can be proposed. Immediately after hole transfer, the electronic configuration resembles a doublet, i.e. $^2\{[Fe^{IV}\text{-}PhAn];MV^{\bullet+}\}$. Hund's rule stipulates that all of the unpaired electrons must have the same spin, and thus, this doublet electronic configuration would rearrange into the corresponding quartet, i.e. $^4\{[Fe^{IV}\text{-}PhAn];MV^{\bullet+}\}$ (**Figure 5**). Amongst the three potential electronic configurations, both the triplet and quartet would lead to spin-forbidden

recombination, whereas recombination from the doublet electronic configuration would be spin-allowed. This combination of potential spin-allowed and spin-forbidden recombination could explain the smaller Φ_{CE} observed for $[Fe(L^{PhAn})_2]^+$ and MV^{2+}. Nevertheless, it should be emphasized that the use of $[Fe(L^{PhAn})_2]^+$ still allows to substantially increase Φ_{CE} of iron-based photosensitizers.

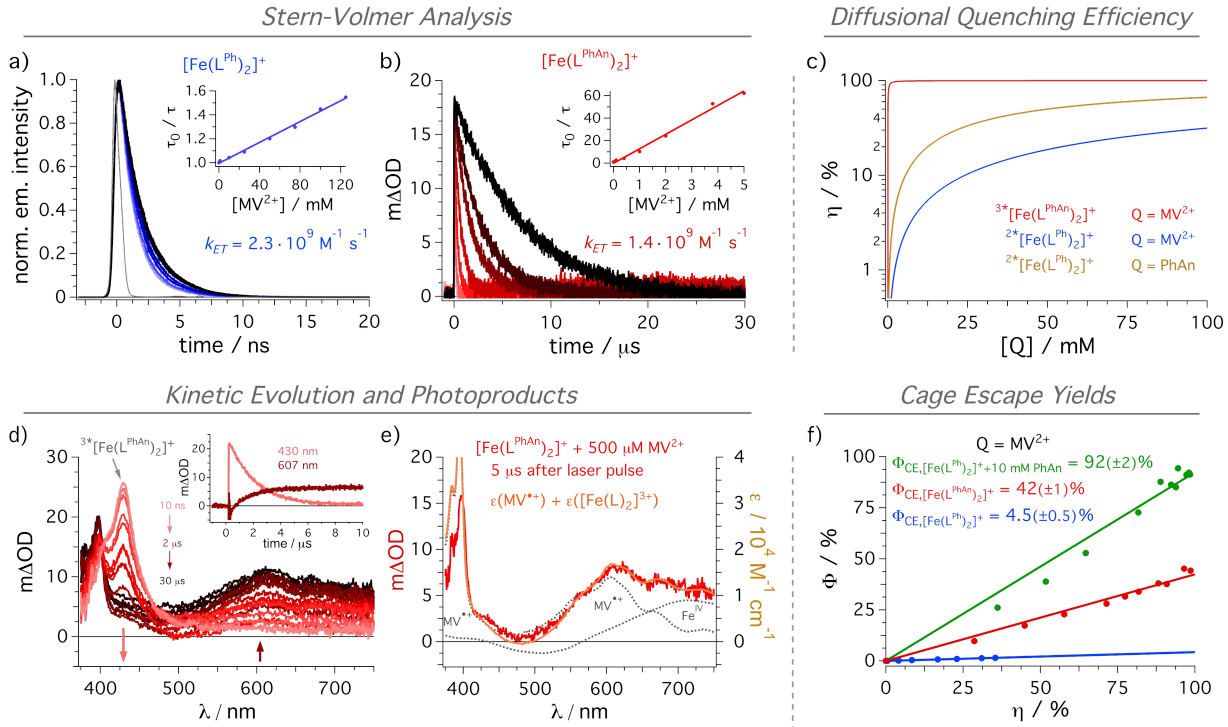

Figure 4. Diffusional excited-state quenching of a) $[Fe(L^{Ph})_2]^+$ and b) $[Fe(L^{PhAn})]^+$ by methyl viologen (MV^{2+}). C) Simulated quenching efficiencies (η) for diffusional excited-state quenching of different iron-based systems with MV^{2+} (blue and red) and PhAn (ocker). d) Nanosecond transient absorption spectroscopy of $[Fe(L^{PhAn})]^+$ in the presence of 500 µM of methyl viologen and e) comparison of the transiently generated photoproducts with electrochemically generated reference spectra. f) Apparent cage escape yield (Φ) for the excited-state quenching by methyl viologen with respect to the excited-state quenching efficiency (η). All spectra were recorded under argon in acetonitrile at room temperature. Further details are provided in the SI.

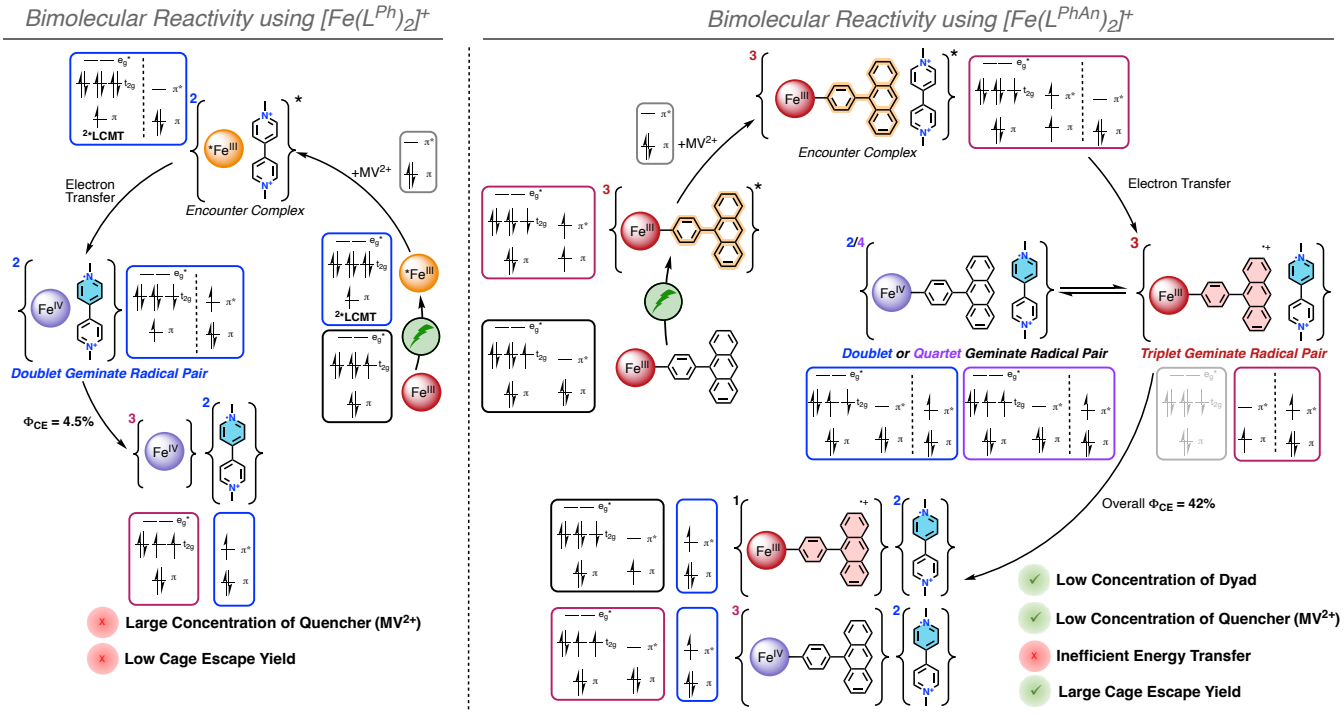

Figure 5. Photophysical scheme associated with the oxidative quenching of $[Fe(L^{Ph})_2]^+$ (left) and $[Fe(L^{PhAn})_2]^+$ (right) alongside the electronic configurations of the relevant species. Note that the electronic configuration between the geminate radical pair and the solvated species is simplified based on Hund's rule. The analogue scheme for the stepwise bimolecular reactivity with PhAn as mediator is presented in section 3.6.2 of the SI.

CONCLUSIONS

In conclusion, we report here the straightforward synthesis of $[Fe(L^{PhAn})_2]^+$, i.e. a dyad composed of a $[Fe(L^{Ph})_2]^+$ core that is further decorated with an anthracene energy acceptor. This "*two birds, one stone*" approach allows not only to extend the excited-state lifetime over three orders of magnitude, but also to drastically improve Φ_{CE} of bimolecular quenching reactions by one order of magnitude. Whereas a solution composed of the individual components, $[Fe(L^{Ph})_2]^+$ and 9-phenylanthracene, led to an appreciable k_q and large Φ_{CE}, it still relied on large concentration of energy acceptor to sufficiently quench the short lifetime of $^{2*}[Fe(L^{PhAn})_2]^+$. On the other hand, $[Fe(L^{PhAn})_2]^+$ provided incomplete energy transfer, where only ~10% of the excited state is transferred to the energy acceptor. The origin of this small energy transfer efficiency is still under investigation and represents a key aspect to improve. Nevertheless, this energy transfer allowed, to the best of our knowledge, for the first time to significantly generate $^1O_2$ using Fe^{III} photosensitizers and to drastically increase Φ_{CE}. Thus, this report represents a key development on the way to place iron photosensitizers as true alternatives in the current photochemical and photophysical landscape.[61-63] Future work will focus on applications as well as investigating the limits of such approach using different energy acceptors with different electronic coupling together with studying the ultrafast dynamics associated with the intramolecular energy transfer processes.

EXPERIMENTAL

Synthesis of $[Fe(L^{Ph})_2](PF_6)$. $L^{Ph}(PF_6)_2$ (1.24 g, 1.95 mmol, 2.1 eq.) was added to a 100 mL Schlenk flask and dried under vacuum at 80°C for 20 hours. Dry THF (40 mL) was added under Argon and the reaction mixture was cooled to –78°C. A solution of LiHMDS (1.09 g, 6.50 mmol, 7.0 eq.) in THF (13 mL) was added slowly and the solution was stirred for 15 minutes and then allowed to warm to room temperature over 30 minutes. A solution of $FeBr_2$ (200 mg, 930 µmol, 1.0 eq.) in THF (35 mL) was sonicated for 20 minutes under Argon and then added slowly to the clear solution of the deprotonated ligand. The reaction mixture was stirred for 20 hours in the dark. Then the solution was exposed to air, inducing a fast color change from black to bright red. The solvent was removed and the residue dissolved in dichloromethane, filtered through a filter frit (POR 3) and the solvent was removed to isolate the crude product. The pure product was isolated after flash column chromatography (neutral Al_2O_3, DCM → DCM/MeCN 5/1) as a dark red solid (248 mg, 927 µmol, 30 %).

^{1}H-NMR (400 MHz, CD_3CN): 14.94 (d, J = 5.2 Hz, 4H), 10.48 (t, J = 5.5 Hz, 4H), 9.81 (t, J = 7.3 Hz, 2H), 4.87 (s, 18H), 1.58 (s, 6H), -12.72 (s, 6H) ppm. These analytical data is in agreement with previously reported characterization data for this compound.[10, 12]

Synthesis of $[Fe(L^{PhBr})_2](PF_6)$. $L^{PhBr}(PF_6)_2$ (1.51 g, 2.15 mmol, 2.2 eq.) was added to a 100 mL Schlenk flask and dried under vacuum at 80°C for 20 hours. Dry THF (45 mL) was added under Argon and the reaction mixture was cooled to –78°C. A solution of LiHMDS (1.21 g, 7.25 mmol, 7.3 eq.) in THF (15 mL) was added dropwise and the solution was stirred for 15 minutes and then allowed to warm to room temperature over 30 minutes. A solution of $FeBr_2$ (215 mg, 1.00 mmol, 1.0 eq.) in THF (40 mL) was sonicated for 20 minutes under Argon and then added slowly to the clear solution of the deprotonated ligand. The reaction mixture was stirred for 20 hours in the dark. Then the solution was exposed to air, inducing a fast color change from black to bright red. The solvent was removed and the residue dissolved in dichloromethane, filtered through a filter frit (POR3) and the solvent was removed to isolate the crude product. The pure product was isolated after flash column chromatography (neutral Al_2O_3, DCM → DCM/MeCN 5/1) as a dark red solid (696 mg,682 µmol, 34 %).

^{1}H-NMR (400 MHz, CD_3CN): 14.83 (d, J = 5.2 Hz, 4H), 10.61 (d, J = 5.3 Hz, 4H), 4.90 (s, 18H), -12.65 (s, 6H) ppm. These analytical data is in agreement with previously reported characterization data for this compound.[53, 64]

Synthesis of $[Fe(L^{PhAn})_2](PF_6).2H_2O$. A 25 mL ACE pressure tube was charged with 9-anthraceneboronic acid (65.0 mg, 294 µmol, 3.0 eq.) and $[Fe(L^{PhBr})_2](PF_6)$ (100 mg, 98.0 µmol, 1.0 eq.). THF (2.25 mL) was added under Argon and the suspension was purged with Argon for 5 minutes. Then $[Pd(PPh_3)_4]$ (11.3 mg, 9.8 µmol, 0.1 eq.) and pre-purged aqueous sodium carbonate solution (2 M, 0.75 mL) were added. The reaction mixture was purged with Argon for another 10 minutes, sealed under Argon and heated to 90 °C for 40 h. The reaction mixture was cooled to room temperature, diluted with water (20 mL), extracted with dichloromethane (3x 50 mL) and the organic phase was dried over anhydrous sodium sulfate. After filtration, the solvent was removed under reduced pressure and the crude red product was filtrated through a short Al_2O_3 column (MeCN → MeCN/water 20/1) and then purified by column chromatography (SiO_2, MeCN/water/sat. aq. KNO_3 20/1/1) and reprecipitated from an aqueous solution with KPF_6 to obtain the desired product (62.3 mg, 51.3 µmol, 52%).

^{1}H NMR (600 MHz, DMSO-d_6) δ 15.13 (s, 4H), 10.54 (s, 4H), 9.95 (d, J = 8.9 Hz, 4H), 9.40 (s, 2H), 8.80 (d, J = 8.9 Hz, 4H), 8.41 (dd, J = 9.0, 4.7 Hz, 4H), 8.15 (dd, J = 8.7, 5.3 Hz, 4H), 5.17 (s, 18H), 1.29 (s, 6H), -12.31 (s, 6H). High resolution ESI-MS m/z calculated for $[C_{64}H_{56}B_2FeN_{12}]^+$ = 1070.42809; found 1070.43006. Elemental Analysis: Anal. Calcd for $C_{64}H_{56}B_2FeN_{12}PF_6.2H_2O$: C, 61.41; H, 4.83; N, 13.43. Found: C, 61.53; H, 4.66; N,12.79

ASSOCIATED CONTENT

Supporting Information

Additional experimental details, Stern-Volmer experiments, photophysical characterization, cage escape yields, transient absorption spectra. The Supporting Information is available free of charge on the ACS Publications website.

AUTHOR INFORMATION

Corresponding Author

Ludovic.Troian@uclouvain.be
Felix.Glaser@uclouvain.be

Author Contributions

The manuscript was written through contributions of all authors. All authors have given approval to the final version of the manuscript.

Funding Sources

Grant no. 40020332 (L.T.-G).

ACKNOWLEDGMENT

This work was supported by the Fonds de la Recherche Scientifique (F.R.S.-FNRS) under grant CDR n°40020332. This publication benefited from the support of the Walloon Region as part of the financing of the FRFS-WEL-T strategic axis. This work was also supported by the "Action de Recherche Concertée" through the project "UNCAGED" under grant no. 23/28-135. L.T.-G. is a Chercheur Qualifié of the Fonds de la Recherche Scientifique – FNRS. F.G. is a chargé de recherches of the Fonds de la Recherche Scientifique – FNRS. F. G., S. D. K. and L.T.-G. gratefully acknowledge the UCLouvain for financial support. The authors warmly acknowledge Prof. Benjamin Elias (and the corresponding U.N021.21 grant) for granting access to the nanosecond transient absorption apparatus. The authors also acknowledge Fabio Lucaccioni (UCLouvain) for his precious assistance in recording elemental analysis.

REFERENCES

1. Prier, C. K.; Rankic, D. A.; MacMillan, D. W. C., Visible Light Photoredox Catalysis with Transition Metal Complexes: Applications in Organic Synthesis. *Chem. Rev.* **2013,** *113*, 5322-5363.
2. Wenger, O. S., Is Iron the New Ruthenium? *Chem-Eur. J.* **2019,** *25*, 6043-6052.
3. Glaser, F.; Aydogan, A.; Elias, B.; Troian-Gautier, L., The Great Strides of Iron Photosensitizers for Contemporary Organic Photoredox Catalysis: On Our Way to the Holy Grail? *Coord. Chem. Rev.* **2024,** *500*, 215522.
4. Förster, C.; Heinze, K., Photophysics and Photochemistry with Earth-Abundant Metals – Fundamentals and Concepts. *Chem. Soc. Rev.* **2020,** *49*, 1057-1070.
5. Reuter, T.; Kruse, A.; Schoch, R.; Lochbrunner, S.; Bauer, M.; Heinze, K., Higher Mlct Lifetime of Carbene Iron(Ii) Complexes by Chelate Ring Expansion. *Chem. Commun.* **2021,** *57*, 7541-7544.
6. Zhang, Y.; Petersen, J. L.; Milsmann, C., A Luminescent Zirconium(Iv) Complex as a Molecular Photosensitizer for Visible Light Photoredox Catalysis. *J. Am. Chem. Soc.* **2016,** *138*, 13115-13118.
7. Zhang, Y.; Lee, T. S.; Favale, J. M.; Leary, D. C.; Petersen, J. L.; Scholes, G. D.; Castellano, F. N.; Milsmann, C., Delayed Fluorescence from a Zirconium(Iv) Photosensitizer with Ligand-to-Metal Charge-Transfer Excited States. *Nature Chem.* **2020,** *12*, 345-352.
8. Chan, A. Y.; Ghosh, A.; Yarranton, J. T.; Twilton, J.; Jin, J.; Arias-Rotondo, D. M.; Sakai, H. A.; McCusker, J. K.; MacMillan, D. W. C., Exploiting the Marcus Inverted Region for First-Row Transition Metal–Based Photoredox Catalysis. *Science* **2023,** *382*, 191-197.
9. Chábera, P.; Liu, Y.; Prakash, O.; Thyrhaug, E.; Nahhas, A. E.; Honarfar, A.; Essén, S.; Fredin, L. A.; Harlang, T. C. B.; Kjær, K. S.*, et al.*, A Low-Spin Fe(Iii) Complex with 100-Ps Ligand-to-Metal Charge Transfer Photoluminescence. *Nature* **2017,** *543*, 695-699.
10. Kjær, K. S.; Kaul, N.; Prakash, O.; Chábera, P.; Rosemann, N. W.; Honarfar, A.; Gordivska, O.; Fredin, L. A.; Bergquist, K.-E.; Häggström, L.*, et al.*, Luminescence and Reactivity of a Charge-Transfer Excited Iron Complex with Nanosecond Lifetime. *Science* **2019,** *363*, 249-253.
11. Rosemann, N. W.; Chábera, P.; Prakash, O.; Kaufhold, S.; Wärnmark, K.; Yartsev, A.; Persson, P., Tracing the Full Bimolecular Photocycle of Iron(Iii)–Carbene Light Harvesters in Electron-Donating Solvents. *J. Am. Chem. Soc.* **2020,** *142*, 8565-8569.
12. Aydogan, A.; Bangle, R. E.; Cadranel, A.; Turlington, M. D.; Conroy, D. T.; Cauët, E.; Singleton, M. L.; Meyer, G. J.; Sampaio, R. N.; Elias, B.*, et al.*, Accessing Photoredox Transformations with an Iron(Iii) Photosensitizer and Green Light. *J. Am. Chem. Soc.* **2021,** *143*, 15661-15673.
13. Aydogan, A.; Bangle, R. E.; De Kreijger, S.; Dickenson, J. C.; Singleton, M. L.; Cauët, E.; Cadranel, A.; Meyer, G. J.; Elias, B.; Sampaio, R. N.*, et al.*, Mechanistic Investigation of a Visible Light Mediated Dehalogenation/Cyclisation Reaction Using Iron(Iii), Iridium(Iii) and Ruthenium(Ii) Photosensitizers. *Catal. Sci. Technol.* **2021,** *11*, 8037-8051.
14. Schwarz, J.; Ilic, A.; Johnson, C.; Lomoth, R.; Wärnmark, K., High Turnover Photocatalytic Hydrogen Formation with an Fe(Iii) N-Heterocyclic Carbene Photosensitiser. *Chem. Commun.* **2022,** *58*, 5351-5354.
15. de Groot, L. H. M.; Ilic, A.; Schwarz, J.; Wärnmark, K., Iron Photoredox Catalysis–Past, Present, and Future. *J. Am. Chem. Soc.* **2023,** *145*, 9369-9388.
16. De Kreijger, S.; Glaser, F.; Troian-Gautier, L., From Photons to Reactions: Key Concepts in Photoredox Catalysis. *Chem Catal.* **2024,** *4*, 101110.
17. Malme, J. T.; Clendening, R. A.; Ash, R.; Curry, T.; Ren, T.; Vura-Weis, J., Nanosecond Metal-to-Ligand Charge-Transfer State in an Fe(Ii) Chromophore: Lifetime Enhancement Via Nested Potentials. *J. Am. Chem. Soc.* **2023,** *145*, 6029-6034.
18. Sinha, N.; Wenger, O. S., Photoactive Metal-to-Ligand Charge Transfer Excited States in 3d6 Complexes with Cr0, Mni, Feii, and Coiii. *J. Am. Chem. Soc.* **2023,** *145*, 4903-4920.
19. Leis, W.; Argüello Cordero, M. A.; Lochbrunner, S.; Schubert, H.; Berkefeld, A., A Photoreactive Iron(Ii) Complex Luminophore. *J. Am. Chem. Soc.* **2022,** *144*, 1169-1173.
20. Witas, K.; Nair, S. S.; Maisuradze, T.; Zedler, L.; Schmidt, H.; Garcia-Porta, P.; Rein, A. S. J.; Bolter, T.; Rau, S.; Kupfer, S.*, et al.*, Beyond the First Coordination Sphere─Manipulating the Excited-State Landscape in Iron(Ii) Chromophores with Protons. *J. Am. Chem. Soc.* **2024,** *146*, 19710-19719.
21. Oppermann, M.; Zinna, F.; Lacour, J.; Chergui, M., Chiral Control of Spin-Crossover Dynamics in Fe(Ii) Complexes. *Nature Chem.* **2022,** *14*, 739-745.
22. Reuter, T.; Zorn, D.; Naumann, R.; Klett, J.; Förster, C.; Heinze, K., A Tetracarbene Iron(Ii) Complex with a Long-Lived Triplet Metal-to-Ligand Charge Transfer State Due to a Triplet-Triplet Barrier. *Angew. Chem. Int. Ed.* **2024,** *63*, e202406438.
23. Dixon, I. M.; Alary, F.; Boggio-Pasqua, M.; Heully, J.-L., Reversing the Relative 3mlct–3mc Order in Fe(Ii) Complexes Using Cyclometallating Ligands: A Computational Study Aiming at Luminescent Fe(Ii) Complexes. *Dalton Trans.* **2015,** *44*, 13498-13503.
24. Giesche, H., Synthesis of Monodispersed Silica Powders I. Particle Properties and Reaction Kinetics. *Journal of the European Ceramic Society* **1994,** *14*, 189-204.
25. Larsen, C. B.; Braun, J. D.; Lozada, I. B.; Kunnus, K.; Biasin, E.; Kolodziej, C.; Burda, C.; Cordones, A. A.; Gaffney, K. J.; Herbert, D. E., Reduction of Electron Repulsion in Highly Covalent Fe-Amido Complexes Counteracts the Impact of a Weak Ligand Field on Excited-State Ordering. *J. Am. Chem. Soc.* **2021,** *143*, 20645-20656.
26. Reinhard, M. E.; Sidhu, B. K.; Lozada, I. B.; Powers-Riggs, N.; Ortiz, R. J.; Lim, H.; Nickel, R.; Lierop, J. v.; Alonso-Mori, R.; Chollet, M.*, et al.*, Time-Resolved X-Ray Emission Spectroscopy and Synthetic High-Spin Model Complexes Resolve Ambiguities in Excited-State Assignments of Transition-Metal Chromophores: A Case Study of Fe-Amido Complexes. *J. Am. Chem. Soc.* **2024,** *146*, 17908-17916.
27. Ortiz, R. J.; Mondal, R.; McCusker, J. K.; Herbert, D. E., Leveraging Intramolecular π-Stacking to Access an Exceptionally Long-Lived 3mc Excited State in an Fe(Ii) Carbene Complex. *J. Am. Chem. Soc.* **2025,** *147*, 1694-1708.
28. Peng, J.; Jiang, X.; Guo, X.; Zhao, D.; Ma, Y., Sensitizer Design for Efficient Triplet–Triplet Annihilation Upconversion: Annihilator-Appended Tris-Cyclometalated Ir(Iii) Complexes. *Chem. Commun.* **2014,** *50*, 7828-7830.

29. Howarth, A. J.; Majewski, M. B.; Wolf, M. O., Photophysical Properties and Applications of Coordination Complexes Incorporating Pyrene. *Coord. Chem. Rev.* **2015,** *282-283*, 139-149.

30. Tyson, D. S.; Bialecki, J.; Castellano, F. N., Ruthenium() Complex with a Notably Long Excited State Lifetime. *Chem. Commun.* **2000**, 2355-2356.

31. Ford, W. E.; Rodgers, M. A. J., Reversible Triplet-Triplet Energy Transfer within a Covalently Linked Bichromophoric Molecule. *J. Phys. Chem* **1992,** *96*, 2917-2920.

32. Sasaki, Y.; Yanai, N.; Kimizuka, N., Osmium Complex–Chromophore Conjugates with Both Singlet-to-Triplet Absorption and Long Triplet Lifetime through Tuning of the Heavy-Atom Effect. *Inorg. Chem.* **2022,** *61*, 5982-5990.

33. Yarnell, J. E.; Deaton, J. C.; McCusker, C. E.; Castellano, F. N., Bidirectional "Ping-Pong" Energy Transfer and 3000-Fold Lifetime Enhancement in a Re(I) Charge Transfer Complex. *Inorg. Chem.* **2011,** *50*, 7820-7830.

34. Kim, D.; Rosko, M. C.; Castellano, F. N.; Gray, T. G.; Teets, T. S., Long Excited-State Lifetimes in Three-Coordinate Copper(I) Complexes Via Triplet–Triplet Energy Transfer to Pyrene-Decorated Isocyanides. *J. Am. Chem. Soc.* **2024,** *146*, 19193-19204.

35. Dierks, P.; Päpcke, A.; Bokareva, O. S.; Altenburger, B.; Reuter, T.; Heinze, K.; Kühn, O.; Lochbrunner, S.; Bauer, M., Ground- and Excited-State Properties of Iron(Ii) Complexes Linked to Organic Chromophores. *Inorg. Chem.* **2020,** *59*, 14746-14761.

36. Campagna, S.; Genovese, S.; Cancelliere, A.; Arrigo, A.; Puntoriero, F., Fe (III) Complexes with Prolonged Luminescence Lifetimes and Symmetry-Breaking Charge Separation. *Research Square*, Submission 2024-04-04, https://doi.org/10.21203/rs.3.rs-4002627/v1, Accessed 2025-02-11.

37. Jiang, T.; Bai, Y.; Zhang, P.; Han, Q.; Mitzi, D. B.; Therien, M. J., Electronic Structure and Photophysics of a Supermolecular Iron Complex Having a Long Mlct-State Lifetime and Panchromatic Absorption. *Proc. Natl. Acad. Sci. USA* **2020,** *117*, 20430-20437.

38. Duncan, T. V.; Ishizuka, T.; Therien, M. J., Molecular Engineering of Intensely near-Infrared Absorbing Excited States in Highly Conjugated Oligo(Porphinato)Zinc−(Polypyridyl)Metal(Ii) Supermolecules. *J. Am. Chem. Soc.* **2007,** *129*, 9691-9703.

39. Duncan, T. V.; Rubtsov, I. V.; Uyeda, H. T.; Therien, M. J., Highly Conjugated (Polypyridyl)Metal−(Porphinato)Zinc(Ii) Compounds: Long-Lived, High Oscillator Strength, Excited-State Absorbers Having Exceptional Spectral Coverage of the near-Infrared. *J. Am. Chem. Soc.* **2004,** *126*, 9474-9475.

40. Goodwin, M. J.; Dickenson, J. C.; Ripak, A.; Deetz, A. M.; McCarthy, J. S.; Meyer, G. J.; Troian-Gautier, L., Factors That Impact Photochemical Cage Escape Yields. *Chem. Rev.* **2024,** *124*, 7379-7464.

41. Wang, C.; Li, H.; Bürgin, T. H.; Wenger, O. S., Cage Escape Governs Photoredox Reaction Rates and Quantum Yields. *Nature Chem.* **2024,** *16*, 1151-1159.

42. Ripak, A.; Vega Salgado, A. K.; Valverde, D.; Cristofaro, S.; de Gary, A.; Olivier, Y.; Elias, B.; Troian-Gautier, L., Factors Controlling Cage Escape Yields of Closed- and Open-Shell Metal Complexes in Bimolecular Photoinduced Electron Transfer. *J. Am. Chem. Soc.* **2024,** *146*, 22818-22828.

43. De Kreijger, S.; Ripak, A.; Elias, B.; Troian-Gautier, L., Investigation of the Excited-State Electron Transfer and Cage Escape Yields between Halides and a Fe(Iii) Photosensitizer. *J. Am. Chem. Soc.* **2024,** *146*, 10286-10292.

44. Wang, C.; Reichenauer, F.; Kitzmann, W. R.; Kerzig, C.; Heinze, K.; Resch-Genger, U., Efficient Triplet-Triplet Annihilation Upconversion Sensitized by a Chromium(Iii) Complex Via an Underexplored Energy Transfer Mechanism. *Angew. Chem. Int. Ed.* **2022,** *61*, e202202238.

45. Han, J.; Jiang, Y.; Obolda, A.; Duan, P.; Li, F.; Liu, M., Doublet–Triplet Energy Transfer-Dominated Photon Upconversion. *J. Phys. Chem. Lett.* **2017,** *8*, 5865-5870.

46. Li, F.; Gillett, A. J.; Gu, Q.; Ding, J.; Chen, Z.; Hele, T. J. H.; Myers, W. K.; Friend, R. H.; Evans, E. W., Singlet and Triplet to Doublet Energy Transfer: Improving Organic Light-Emitting Diodes with Radicals. *Nature Comm.* **2022,** *13*, 2744.

47. Wellauer, J.; Ziereisen, F.; Sinha, N.; Prescimone, A.; Velić, A.; Meyer, F.; Wenger, O. S., Iron(Iii) Carbene Complexes with Tunable Excited State Energies for Photoredox and Upconversion. *J. Am. Chem. Soc.* **2024,** *146*, 11299-11318.

48. O'Shea, J. M.; Yun, Y. J.; Jamhawi, A. M.; Peccati, F.; Jiménez-Osés, G.; Ayitou, A. J.-L., Doublet Spin State Mediated Photoluminescence Upconversion in Organic Radical Donor-Triplet Acceptor Dyads. *J. Am. Chem. Soc.* **2025,** *147*, 1017-1027.

49. Jin, P.; Xu, X.; Yan, Y.; Hammecke, H.; Wang, C., Luminescent Fe(Iii) Complex Sensitizes Aerobic Photon Upconversion and Initiates Photocatalytic Radical Polymerization. *J. Am. Chem. Soc.* **2024,** *146*, 35390-35401.

50. Neumann, S.; Wenger, O. S.; Kerzig, C., Controlling Spin-Correlated Radical Pairs with Donor–Acceptor Dyads: A New Concept to Generate Reduced Metal Complexes for More Efficient Photocatalysis. *Chem-Eur. J.* **2021,** *27*, 4115-4123.

51. Sell, A. C.; Wetzel, J. C.; Schmitz, M.; Maijenburg, A. W.; Woltersdorf, G.; Naumann, R.; Kerzig, C., Water-Soluble Ruthenium Complex-Pyrene Dyads with Extended Triplet Lifetimes for Efficient Energy Transfer Applications. *Dalton Trans.* **2022,** *51*, 10799-10808.

52. Olmsted, J.; Meyer, T. J., Factors Affecting Cage Escape Yields Following Electron-Transfer Quenching. *J. Phys. Chem* **1987,** *91*, 1649-1655.

53. Prakash, O.; Lindh, L.; Kaul, N.; Rosemann, N. W.; Losada, I. B.; Johnson, C.; Chábera, P.; Ilic, A.; Schwarz, J.; Gupta, A. K.*, et al.*, Photophysical Integrity of the Iron(Iii) Scorpionate Framework in Iron(Iii)–Nhc Complexes with Long-Lived 2lmct Excited States. *Inorg. Chem.* **2022,** *61*, 17515-17526.

54. Suzuki, K.; Kobayashi, A.; Kaneko, S.; Takehira, K.; Yoshihara, T.; Ishida, H.; Shiina, Y.; Oishi, S.; Tobita, S., Reevaluation of Absolute Luminescence Quantum Yields of Standard Solutions Using a Spectrometer with an Integrating Sphere and a Back-Thinned Ccd Detector. *Phys. Chem. Chem. Phys.* **2009,** *11*, 9850-9860.

55. Montalti, M.; Credi, A.; Prodi, L.; Gandolfi, M. T., *Handbook of Photochemistry*. CRC Press: 2006.

56. Murov, S. L.; Carmichael, I.; Hug, G. L., *Handbook of Photochemistry, 2nd Edition*. Marcel Dekker, Inc.,New York: 1993.

57. Takizawa, S.-y.; Aboshi, R.; Murata, S., Photooxidation of 1,5-Dihydroxynaphthalene with Iridium Complexes as Singlet Oxygen Sensitizers. *Photochem. Photobio. Sci.* **2011,** *10*, 895-903.

58. Chen, K.-K.; Guo, S.; Liu, H.; Li, X.; Zhang, Z.-M.; Lu, T.-B., Strong Visible-Light-Absorbing Cuprous Sensitizers for Dramatically Boosting Photocatalysis. *Angew. Chem. Int. Ed.* **2020,** *59*, 12951-12957.

59. Schmitz, M.; Bertrams, M.-S.; Sell, A. C.; Glaser, F.; Kerzig, C., Efficient Energy and Electron Transfer Photocatalysis with a Coulombic Dyad. *J. Am. Chem. Soc.* **2024,** *146*, 25799-25812.

60. Wilson, G. J.; Launikonis, A.; Sasse, W. H. F.; Mau, A. W. H., Chromophore-Specific Quenching of Ruthenium Trisbipyridine−Arene Bichromophores by Methyl Viologen. *J. Phys. Chem. A* **1998,** *102*, 5150-5156.

61. Dutta, S.; Erchinger, J. E.; Strieth-Kalthoff, F.; Kleinmans, R.; Glorius, F., Energy Transfer Photocatalysis: Exciting Modes of Reactivity. *Chem. Soc. Rev.* **2024,** *53*, 1068-1089.

62. Strieth-Kalthoff, F.; Glorius, F., Triplet Energy Transfer Photocatalysis: Unlocking the Next Level. *Chem* **2020,** *6*, 1888-1903.

63. Neveselý, T.; Wienhold, M.; Molloy, J. J.; Gilmour, R., Advances in the E → Z Isomerization of Alkenes Using Small Molecule Photocatalysts. *Chem. Rev.* **2022,** *122*, 2650-2694.

64. Ripak, A.; De Kreijger, S.; Sampaio, R. N.; Vincent, C. A.; Cauët, É.; Jabin, I.; Tambar, U. K.; Elias, B.; Troian-Gautier, L., Photosensitized Activation of Diazonium Derivatives for C–B Bond Formation. *Chem Catal.* **2023,** *3*, 100490.

TOC Graphic

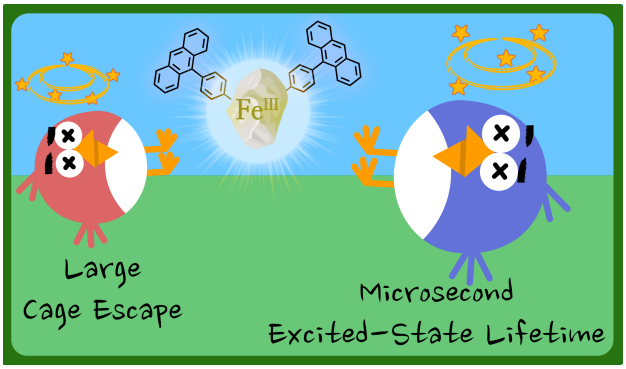
Fe^{III}
Large
Cage Escape
Microsecond
Excited-State Lifetime